

Polarized deep inelastic scattering at low Bjorken x and resummation of logarithmic corrections, $\ln^2(1/x)$.

Beata Ziaja ^{† 1}

[†] *Department of Theoretical Physics, Institute of Nuclear Physics,
Radzikowskiego 152, 31-342 Cracow, Poland*

Dedicated to Professor Jan Kwieciński in honour of his 65th birthday

Abstract:

For an accurate description of the polarized deep inelastic scattering at low x including the logarithmic corrections, $\ln^2(1/x)$, is required. These corrections resummed strongly influence the behaviour of the spin structure functions and their moments. Results of the work of J. Kwieciński and myself on this problem are reviewed.

1. Introduction

The problem of identifying the spin components of the polarized nucleon has been attracting the attention of the high-energy community since many years [1, 2, 3, 4]. The data obtained in 1988 by the EMC collaboration [5] showed that the total participation of quarks in the proton spin was very small. This contradicted theoretical predictions, obtained with the well-founded Ellis-Jaffe sum rule [3, 4]. That sum rule connected the moments of quark distributions to the nucleon axial coupling constants. Following that rule, the quarks should participate in about three-fifth of the total nucleon spin with the parton quark model. The discrepancy between the theoretical expectations and the experimental data for the polarized proton has been often referred as the "puzzle of the proton spin" [2].

Since 1988 several observations contributing to this problem have been made. New experimental data were collected. They showed that neglecting the participation of the strange quarks at the Ellis-Jaffe sum rule was not correct [3, 2].

A significant progress in the theoretical analysis of the nucleon spin structure function has been also made. A derivation of g_1 in the subleading approximation of the quantum chromodynamics (NLO DGLAP) showed a difficulty with the unique defining the quark component of the polarized nucleon. In the standard \overline{MS} factorization scheme at the NLO QCD [6, 7] the first moment of the singlet parton distribution, $\Delta\Sigma(Q^2)$, is not conserved. The singlet moments calculated at different factorization schemes differ by a term, $\widetilde{\alpha}_s(Q^2) \int_0^1 dx \Delta g(x, Q^2) \sim O(\alpha_s^0)$, which can be large even at $Q^2 \rightarrow \infty$. This is a direct consequence of the axial anomaly [8, 9, 2]. Therefore the differences between the quark moments

¹ e-mail: ziaja@unix.tsl.uu.se

at different schemes can be large. This makes the physical interpretation of these moments difficult.

It is also not clear how the orbital angular momentum, L , participates in the total nucleon spin [2]. Again, there is a problem with the unique definition of this momentum. The total angular momenta of quarks and gluons, J_q and J_g , are well defined and gauge invariant. However, separation of their spin and orbital components is not unique. It depends on the gauge transformation used.

New experiments emerge, and they will possibly help explaining the puzzle of the nucleon spin. The data from the region of low values of Bjorken x , $x < 10^{-3}$, will be of special importance. Theoretical predictions show that at low x the structure function, $g_1(x, Q^2)$, is influenced by large logarithmic corrections, $\ln^2(1/x)$, [10, 11]. As a consequence, large contributions to the moments of the structure functions from this region are expected [10, 11, 12, 13, 14, 15, 16]. Including the region of low x into the experimental analysis will improve the estimation of the parton contributions to the nucleon spin. This may lead to a better understanding the spin components of the nucleon.

In Refs. [16, 17, 18, 19] we investigated how those logarithmic corrections, $\ln^2(1/x)$, influenced the spin structure function, g_1 , at low values of Bjorken x . We formulated the evolution equations for the unintegrated parton distributions which included the complete resummation of the double logarithmic contributions, $\ln^2(1/x)$. Afterwards, those equations were completed with the standard LO DGLAP evolution terms, in order to obtain the proper behaviour of the parton distributions at the moderate and large values of x .

The equations obtained were applied to the following observables and processes: (i) to the nucleon structure function, g_1 , in the polarized deep inelastic scattering, (ii) to the structure function of the polarized photon, g_1^γ , in the scattering of a lepton on a polarized photon, and (iii) to the differential structure function, $x_J \partial^2 g_1 / \partial x_J \partial k_J^2$, in the polarized deep inelastic scattering accompanied by a forward jet. Case (iii) was proposed to be a test process for the presence and the magnitude of the $\ln^2(1/x)$ contributions. For each process the consequences of including the logarithmic corrections were studied in a detail.

Finally, some predictions for the observables, the asymmetry and the cross sections, in the processes (i)-(iii) were obtained. They were important to planned experiments with the polarized HERA and linear colliders, which would probe the region of low values of Bjorken x .

2. Nucleon spin structure function, g_1

The total cross section for the polarized deep inelastic scattering is expressed by a contraction of two tensors: the leptonic tensor, $L_{\mu\nu}$ and the hadronic tensor, $W^{\mu\nu}$, $\sigma \sim L_{\mu\nu} W^{\mu\nu}$ [1]. The hadronic tensor can be expanded in terms of the Lorentz invariants, and the expansion

coefficients define measurable structure functions [1,4]. The spin structure function, g_1 , is an expansion coefficient at the asymmetric spin term, $\epsilon^{\mu\nu\rho\sigma} q_\rho S_\sigma$, where q denotes the momentum transfer, and S is a polarization vector of the nucleon.

At low values of Bjorken x the asymptote of g_1 predicted by the Regge model shows a weak scaling with x [20,21]:

$$g_1^i(x, Q^2) = \gamma_i(Q^2) x^{-\alpha_i(0)}, \quad (1)$$

where $g_1^i(x, Q^2)$ is either a singlet ($i = S$) or a non-singlet ($i = NS$) combination of the nucleon structure functions, g_1^p and g_1^n . It is expected that $\alpha_{S,NS}(0) \leq 0$ and that $\alpha_S(0) \approx \alpha_{NS}(0)$ i.e. the singlet spin structure function with the Regge model is expected to show similar behaviour at low x as the non-singlet one [16].

The asymptotic form of g_1 obtained with the standard DGLAP evolution in QCD is more singular than this obtained with the Regge model [10,11].

However, these predictions do not involve the contribution of the logarithms, $\ln(1/x)$, which is significant at low x . In the unpolarized DIS the resummation of the logarithms, $\ln(1/x)$, was performed by the BFKL equation [22,23]. The analysis of the polarized DIS showed that at low x the structure function of the polarized nucleon, $g_1(x, Q^2)$, was influenced by large double logarithmic corrections, $\ln^2(1/x)$, [10,11]. Those corrections originated from the ladder diagrams and the nonladder ("bremsstrahlung") diagrams with the requirement of ordering the ratios, k_n^2/x_n , for the exchanged partons [10,11,24,25]. The momentum, k_n , was the transverse momentum, and the fraction, x_n , was the longitudinal momentum fraction of the n th parton exchanged. Ladder diagrams corresponded to the diagrams describing the forward scattering of a photon on a nucleon with a ladder of partons radiatively generated [10,11,15]. Nonladder diagrams were the ladder diagrams of the forward γN scattering with some extra parton propagators attached. They were resummed with the infrared evolution equation [24,25].

Those logarithmic corrections were studied in a detail in Refs. [16,15]. Recursive equations for the resummation of the double logarithmic contributions were there formulated, both for the singlet and the nonsinglet component of g_1 . Those equations transformed to the moment space gave proper anomalous dimensions as derived from the infrared evolution equations [24,25,16].

The resummation of $\ln^2(1/x)$ was performed for the unintegrated parton distributions, f_i ($i = S, NS, g$). Therefore the ordering requirement, $k_n^2/x_n < k_{n+1}^2/x_{n+1}$, for the exchanged partons was naturally included into the evolution equations. Moreover, the evolution $\ln^2(1/x)$ was included into the equation kernels, and the nonperturbative input was separated as an inhomogeneous term. This allowed for including the kernels of the standard DGLAP evolution into the equations, which was necessary, in order to obtain a proper behaviour of the parton distributions at moderate and large values of x .

The full (unified) equation for the nonsinglet unintegrated parton distribution, f_{NS} was:

$$\begin{aligned}
f_{NS}(x, Q^2) = & \widetilde{\alpha}_s(Q^2)(\Delta P \otimes \Delta q_{NS}^{(0)})(x) + \widetilde{\alpha}_s(Q^2) \int_{k_0^2}^{Q^2} \frac{dk^2}{k^2} (\Delta P \otimes f_{NS})(x, k^2) \\
& \text{(DGLAP)} \\
& + \widetilde{\alpha}_s(Q^2) \frac{4}{3} \int_x^1 \frac{dz}{z} \int_{Q^2}^{Q^2/z} \frac{dk^2}{k^2} f_{NS}\left(\frac{x}{z}, k^2\right) \\
& \text{(Ladder)} \\
& - \widetilde{\alpha}_s(Q^2) \int_x^1 \frac{dz}{z} \left(\left[\frac{\tilde{\mathbf{F}}_8}{\omega^2} \right](z) \frac{\mathbf{G}_0}{2\pi^2} \right)_{qq} \int_{k_0^2}^{Q^2} \frac{dk^2}{k^2} f_{NS}\left(\frac{x}{z}, k^2\right) \\
& - \widetilde{\alpha}_s(Q^2) \int_x^1 \frac{dz}{z} \int_{Q^2}^{Q^2/z} \frac{dk^2}{k^2} \left(\left[\frac{\tilde{\mathbf{F}}_8}{\omega^2} \right] \left(\frac{k^2}{Q^2} z \right) \frac{\mathbf{G}_0}{2\pi^2} \right)_{qq} f_{NS}\left(\frac{x}{z}, k^2\right). \\
& \text{(Nonladder)}
\end{aligned} \tag{2}$$

For a detailed form of the kernels see Appendix A. Matrices, \mathbf{F}_8 and \mathbf{G}_0 , represent the octet partial waves and the colour factors respectively. They are described in a detail in Appendix A. Symbol $\left[\widetilde{\mathbf{F}}_8/\omega^2 \right](z)$ denotes the inverse Mellin transform of \mathbf{F}_8/ω^2 :

$$\left[\widetilde{\mathbf{F}}_8/\omega^2 \right](z) = \int_{\delta-i\infty}^{\delta+i\infty} \frac{d\omega}{2\pi i} z^{-\omega} \mathbf{F}_8(\omega)/\omega^2. \tag{3}$$

with the integration contour located to the right of the singularities of the function $\mathbf{F}_8(\omega)/\omega^2$.

The singlet distribution, $f_S = \begin{pmatrix} f_\Sigma \\ f_g \end{pmatrix}$, was resummed by a similar vector equation, formulated for the quark and the gluon components [16].

The integrated parton distributions, $\Delta q_i(x, Q^2)$, were obtained with the unintegrated ones, using the relation:

$$\Delta q_i(x, Q^2) = \Delta q_i^{(0)}(x) + \int_{k_0^2}^{W^2} \frac{dk^2}{k^2} f_i(x' = x(1 + \frac{k^2}{Q^2}), k^2), \tag{4}$$

where the phase-space was extended from Q^2 to $W^2 = Q^2(1/x - 1)$ corresponding to the total energy squared measured in the center-of-mass frame [15]. The index, $i = S, NS, g$, and $\Delta q_i^{(0)}(x)$ was the input parton distribution including the contributions from the nonperturbative region.

Finally, the structure function, g_1 , at the LO accuracy was:

$$g_1(x, Q^2) = \frac{\langle e^2 \rangle}{2} \left\{ \Delta q_{NS}(x, Q^2) + \Delta q_S(x, Q^2) \right\}, \tag{5}$$

where $\langle e^2 \rangle = \frac{1}{N_f} \sum_{l=1}^{N_f} e_l^2$, and N_f denoted the number of active flavours ($N_f = 3$).

The analysis of g_1 obtained with the unified evolution including the DGLAP terms at the LO accuracy was performed in [16]. The results obtained with the standard LO DGLAP

evolution and the unified evolution (DL+LO DGLAP) were similar at $x > 10^{-3}$. Significant discrepancies appeared at very low x , $x < 10^{-4}$, when the corrections, $\ln^2(1/x)$, were predominant (Fig. 1).

For the gluon distribution, Δg , the discrepancies between the LO DGLAP and DL+LO DGLAP curves were large (Fig. 2). This shows that the unified evolution of gluon distribution is driven by the ladder and the nonladder terms.

Recently, the unified equation were completed by the NLO DGLAP terms [26, 27]. The relations between the NLO DGLAP and the DL+NLO DGLAP curves of Refs. [26, 27] were similar as the relations between the LO DGLAP and the DL+NLO DGLAP curves obtained in [16].

3. Spin structure of the polarized photon

Unified evolution equations may be also applied to investigate the structure of the polarized photon in a deep inelastic scattering of an electron on photon beams [17]. The spin structure function of the polarized photon, g_1^γ , will be measured with future linear colliders e^+e^- and $e\gamma$ [28, 29, 30]. In particular, the scattering $e\gamma$ will probe the g_1^γ at low values of Bjorken x . The partonic content of the polarized photon can be also measured with the process of the dijet photoproduction at the scattering of an electron on a proton [31].

Using the unified equations for the description of $e\gamma$ scattering requires an extra inhomogeneous term, $\Delta k_i(x, Q^2)$, to be included into these equations. This term describes the pointlike coupling of the photon to quarks, antiquarks and gluons [28]. It joins the DGLAP evolution equations in the following way:

$$\frac{d}{d \ln Q^2} \Delta q_i(x, Q^2) = \Delta k_i(x, Q^2) + \widetilde{\alpha}_s(Q^2) (\Delta P \otimes \Delta q_i)(x, Q^2), \quad (6)$$

where $i = S, NS, g$. There is no photon-gluon coupling at the LO of DGLAP, $\Delta k_g(x, Q^2) = 0$ [28].

In Ref. [17] we found an analytic solution of the simplified evolution equations. They described the DL evolution in an approximation, where the nonladder terms were neglected. We got the asymptotic form of g_1^γ at the limit, $x \rightarrow 0$. As expected, g_1^γ scaled with x . The scaling coefficient was negative, and it was related in a simple way to the asymptotic scaling coefficients of the nucleon structure function, g_1 .

Then we found a numerical solution for g_1^γ with the full evolution equations, taking into account the standard DGLAP evolution at the LO accuracy. The input parametrization fulfilled the sum rule for g_1^γ [32, 33]:

$$\int_0^1 dx g_1^\gamma(x, Q^2) = 0. \quad (7)$$

We considered two limiting cases for the input parametrization of the quark and gluon distributions: (i) the case, when $\Delta q^{(0)} = 0$ and $\Delta g^{(0)} = 0$, and the solutions of the evolution equations were generated radiatively from the inhomogeneous terms, Δk , (ii) the case, when $\Delta q^{(0)} = 0$ but the gluon input was nonzero. In that case the input parametrization of gluon distribution was obtained with the vector-meson-dominance model (VMD), assuming the dominance of the mesons, ρ and ω [34, 35].

Including the double logarithmic corrections significantly influenced the behaviour of g_1^γ . The differences between the curves obtained with the LO DGLAP, NLO DGLAP and DL+LO DGLAP evolution strongly depended on the input parametrization of the parton distributions used (Figs. 3,4). It depended also on the infrared cut-off, k_0^2 (not shown). However, the estimated value of asymmetry, g_1^γ/F_1^γ was small, $\sim 10^{-3}$ at $x = 10^{-4}$, i.e. it was difficult to measure.

The gluon distribution, Δg , obtained strongly depended on the input parametrization used (Figs. 5,6). In case (i) Δg was negative at low values of x , in case (ii) it was positive. Future experiments will be then able to determine which parametrization is correct.

4. Logarithmic corrections tested

The presence and the magnitude of the logarithmic corrections, $\ln^2(1/x)$, can be tested in the polarized deep inelastic scattering accompanied by a forward jet. This idea was first applied for testing the BFKL resummation in the unpolarized DIS [36, 37].

Assume, that a forward jet is produced in the DIS of an electron on a proton. The momentum coordinates of the jet are, (x_J, k_J^2) , where x_J is the longitudinal momentum fraction, and k_J^2 denotes the transverse momentum of the jet squared. The momentum transfer carried by the photon is q , and the Bjorken variable x is defined as: $x = Q^2/(2pq)$, where $Q^2 = -q^2$ and p is the momentum of the proton.

If the jet coordinates fulfill the requirement:

$$\begin{aligned} x_J &\gg x, \\ k_J^2 &\sim Q^2, \end{aligned} \tag{8}$$

the jet is produced at low values of x/x_J . A contribution to this process coming from the standard DGLAP evolution is then suppressed ($k_J^2 \sim Q^2$) [36, 37, 38, 39, 40, 41], and the nonperturbative region is unpenetrated by the evolution, $\ln^2(1/x)$ [42, 43].

In this process we measure the differential cross section. It is related to the momentum transfer, Q^2 , the electron energy fraction, y , and the differential structure function $x_J \partial^2 g_1 / \partial x_J \partial k_J^2$. In analogy to the full structure function, g_1 , the differential structure function may be expressed through the integrated parton distributions in a proton and the unintegrated distributions of quarks and antiquarks in a parton [18].

In Ref. [18] we formulated the $\ln^2(1/x)$ evolution equations for the unintegrated distributions of (anti)quarks in a parton. In those equations we included the leading ladder terms, and neglected the subleading ones. We neglected also the DGLAP terms as the DGLAP evolution was suppressed [18]. We found an analytic solution of those equations in the following cases: (i) for the fixed coupling constant, $\alpha_s(\mu^2)$, where $\mu = (k_J^2 + Q^2)/2$ [38, 39], (ii) for the running coupling constant, $\alpha_s(\mu^2)$, where $\mu^2 = k_f^2/\zeta$, and k_f^2 denotes the transverse momentum of (anti)quark squared, and ζ is its longitudinal momentum fraction. After numerical integrating the unintegrated distributions we got the differential structure function, $x_J \partial^2 g_1 / \partial x_J \partial k_J^2$ (Figs. 7,8). This function strongly changed with the value of the ratio, x/x_J , and it depended also on the transverse momentum of the jet, k_J^2 . The strong dependence on x/x_J was a direct effect of the logarithmic resummation. Comparing the results, we found that the case (ii) with the running coupling constant was more realistic than the case (i) with the fixed coupling constant. In both cases the $\ln^2(1/x)$ effects were much larger than the background described by the Born approximation (not shown).

In Ref. [19] we estimated the cross section and the asymmetry for the DIS accompanied by a forward jet. We used the kinematical cuts as planned for the future collider, the polarized HERA [44, 45, 46]. The effects of $\ln^2(1/x)$ resummation contributed significantly to the asymmetric cross section $d\sigma/dx$, where x was the Bjorken variable (Fig. 9). The asymmetry obtained was, however, small, and changed between -0.01 and -0.04 at low x .

5. Summary

We performed the analysis of the polarized deep inelastic scattering in the region of low values of Bjorken x . We used the evolution equations formulated for the unintegrated parton distributions. Those equations included the complete resummation of the double logarithmic contributions, $\ln^2(1/x)$, and the standard LO DGLAP evolution terms. The DGLAP evolution was included into those equations, in order to obtain the proper behaviour of the parton distributions at the moderate and large values of x .

Using that formalism, we obtained predictions for the following observables: (i) the nucleon structure function, g_1 , in the polarized deep inelastic scattering, (ii) the structure function of the polarized photon, g_1^γ , in the scattering of a lepton on a polarized photon, and (iii) the differential structure function, $x_J \partial^2 g_1 / \partial x_J \partial k_J^2$, in the polarized deep inelastic scattering accompanied by a forward jet.

For each process the consequences of including the logarithmic corrections were studied in a detail. Generally, we observed an enhancement of the magnitude of g_1^p , g_1^γ and Δg obtained with the unified evolution as compared to the pure LO DGLAP results. Especially, the behaviour of gluon distributions with the unified evolution at low x was clearly dominated by the large contribution of the ladder and nonladder terms. Some predictions for the observ-

ables, the asymmetry and the cross sections, in the processes (i)-(iii) were also obtained. The case (iii) tested the presence and the magnitude of the $\ln^2(1/x)$ contributions in DIS. In that case the asymmetry parameter estimated with the kinematical cuts of the future collider, polarized HERA, was between -0.04 and -0.01 at low x .

To sum up, our observations suggest that the standard DGLAP evolution is not complete at low x , where the effects of $\ln^2(x)$ resummation are large and therefore cannot be neglected. This result is important to planned experiments with the polarized HERA and linear colliders, which would probe the region of low values of Bjorken x .

Acknowledgements

I would like to express my deep gratitude to Professor Jan Kwieciński who introduced me into the spin physics, who inspired and supported my research in this field. I learned from him so much.

This research has been supported in part by the Polish State Committee for Scientific Research with grants 2 P03B 05119, 2P03B 14420, and European Community grant 'Training and Mobility of Researchers', Network 'Quantum Chromodynamics and the Deep Structure of Elementary Particles' FMRX-CT98-0194.

Appendix A

Here a brief description of the evolution kernels of Eq. (2) is given. DGLAP kernels were taken from Ref. [1]. Here the DGLAP kernel ΔP includes only the LO terms:

$$\Delta P = \Delta P^{(0)}. \quad (9)$$

The ladder kernels corresponding to the LO DGLAP kernels at the longitudinal momentum transfer, $z = 0$, [16] generate the double logarithmic corrections in the region of $Q^2 < k^2 < Q^2/z$.

The nonladder kernels were obtained in Ref. [16] from the infrared evolution equations written for the singlet partial waves $\mathbf{F}_0, \mathbf{F}_8$ [10, 11, 24, 25]. In [16] we noticed that extending the kernel of the double logarithmic evolution equations from the ladder one,

$$\widetilde{\alpha}_s(Q^2) \Delta P_{qq}/\omega, \quad (10)$$

to the modified one,

$$\widetilde{\alpha}_s(Q^2) \left(\Delta P_{qq}/\omega - (\mathbf{F}_8(\omega) \mathbf{G}_0)_{qq}/(2\pi^2\omega^2) \right), \quad (11)$$

gave a proper anomalous dimension as derived from the infrared evolution equations.

Matrix \mathbf{G}_0 contained colour factors resulting from attaching the soft gluon to external legs of the scattering amplitude :

$$\mathbf{G}_0 = \begin{pmatrix} \frac{N^2-1}{2N} & 0 \\ 0 & N \end{pmatrix}, \quad (12)$$

where N was the number of colours.

Further, it was checked that the Born approximation of \mathbf{F}_8 ,

$$\mathbf{F}_8^{Born}(\omega) \approx 8\pi^2 \widetilde{\alpha}_s(Q^2) \frac{\mathbf{M}_8}{\omega}. \quad (13)$$

gave accurate results for the DL evolution. Matrix \mathbf{M}_8 was a splitting function matrix in the colour octet t -channel,

$$\mathbf{M}_8 = \begin{pmatrix} -\frac{1}{2N} & -\frac{N_F}{2} \\ N & 2N \end{pmatrix}. \quad (14)$$

The inverse Mellin transform of $\mathbf{F}_8^{Born}(\omega)$ then read :

$$\left[\frac{\tilde{\mathbf{F}}_8^{Born}}{\omega^2} \right](z) = 4\pi^2 \widetilde{\alpha}_s(Q^2) \mathbf{M}_8 \ln^2(z). \quad (15)$$

The evolution equation (2) includes the nonladder corrections in the Born approximation (15).

References

- [1] B. Lampe and E. Reya. *Phys.Rept.*, 332:1, 2000.
- [2] H.-Y. Cheng. *Chin. J. Phys.*, 38:753, 2000.
- [3] M. C. Vetterli. *hep-ph/9812420*.
- [4] B. L. Ioffe. *Surveys High Energ. Phys.*, 8:107, 1995.
- [5] J. Ashman et al. EMC. *Phys. Lett. B*, 206:364, 1988.
- [6] R. Mertig and W. L. van Neerven. *Z. Phys. C*, 70:637, 1996.
- [7] W. Vogelsang. *Phys. Rev. D*, 54:2023, 1996.
- [8] R. D. Carlitz, J. C. Collins, and A. H. Mueller. *Phys. Lett. B*, 214:229, 1988.
- [9] E. Leader, A. V. Sidorov, and D. B. Stamenov. *Phys. Lett. B*, 445:232, 1998.
- [10] J. Bartels, B. I. Ermolaev, and M. G. Ryskin. *Z. Phys. C*, 70:273, 1996.
- [11] J. Bartels, B. I. Ermolaev, and M. G. Ryskin. *Z. Phys. C*, 72:627, 1996.
- [12] J. Blümlein and A. Vogt. *Acta Phys. Pol. B*, 27:1309, 1996.
- [13] J. Blümlein and A. Vogt. *Phys. Lett. B*, 386:350, 1996.
- [14] Y. Kiyo, J. Kodaira, and H. Tochimura. *Z. Phys. C*, 74:631, 1997.
- [15] B. Badelek and J. Kwieciński. *Phys. Lett. B*, 418:229, 1998.

- [16] J. Kwieciński and B. Ziaja. *Phys. Rev. D*, 60:054004, 1999.
- [17] J. Kwieciński and B. Ziaja. *Phys. Rev. D*, 63:054022, 2001.
- [18] J. Kwieciński and B. Ziaja. *Phys. Lett. B*, 464:293, 1999.
- [19] J. Kwieciński and B. Ziaja. *Phys. Lett. B*, 470:247, 1999.
- [20] B. L. Ioffe, V. A. Khoze, and L. N. Lipatov. *Hard Processes. North-Holland, Amsterdam*, 1984.
- [21] J. Ellis and M. Karliner. *Phys. Lett. B*, 213:73, 1988.
- [22] E. A. Kuraev, L. N. Lipatov, and V. Fadin. *Sov. Phys. JETP*, 45:199, 1977.
- [23] Y. Y. Balitsky and L. N. Lipatov. *Sov. J. Nucl. Phys.*, 28:822, 1978.
- [24] R. Kirschner and L. N. Lipatov. *Nucl. Phys. B*, 213:122, 1983.
- [25] R. Kirschner. *Z. Phys. C*, 67:459, 1995.
- [26] B. Ziaja. *Phys. Rev. D*, 66:114017, 2002.
- [27] B. Ziaja. *to be published in Eur. Phys. J. C*, 2003.
- [28] M. Stratmann and W. Vogelsang. *Phys. Lett. B*, 386:370, 1996.
- [29] M. Stratmann. *Nucl. Phys. B (Proc. Suppl.)*, 82:400, 2000.
- [30] A. Vogt. *Nucl. Phys. B (Proc. Suppl.)*, 82:394, 2000.
- [31] M. Stratmann and W. Vogelsang. Towards the parton densities of polarized photons at HERA. **Hamburg 1999, Polarized protons at high energies - Accelerator challenges and physics opportunities**, page 324, 1999.
- [32] S. D. Bass. *Int. J. Mod. Phys. A*, 7:6039, 1992.
- [33] S. Narison, G. M. Shore, and G. Veneziano. *Nucl. Phys. B*, 391:69, 1993.
- [34] J. J. Sakurai. *Ann. Phys.*, 11:1, 1960.
- [35] T. T. Bauer et al. *Rev. Mod. Phys.*, 50:261, 1978.
- [36] A. Mueller. *Nucl. Phys. (Proc. Suppl.)*, 18C:125, 1990.
- [37] A. Mueller. *J. Phys. G*, 17:1443, 1991.
- [38] J. Bartels, A. De Roeck, and M. Loewe. *Z. Phys. C*, 54:635, 1992.
- [39] W. K. Tang. *Phys. Lett. B*, 278:363, 1992.
- [40] J. Kwieciński, A. D. Martin, and P. J. Sutton. *Phys. Rev. D*, 46:921, 1992.
- [41] J. Kwieciński, A. D. Martin, and P. J. Sutton. *Phys. Lett. B*, 287:254, 1992.
- [42] J. Bartels and H. Lotter. *Phys. Lett. B*, 309:400, 1993.
- [43] J. Bartels. *J. Phys. G*, 19:1611, 1993.
- [44] C. Adloff et al. H1 Collaboration. *Nucl. Phys. B*, 538:3, 1999.
- [45] ZEUS Collaboration. *Eur. Phys. J. C*, 6:239, 1999.
- [46] A. De Roeck. *Acta Phys. Pol. B*, 29:1343, 1998.

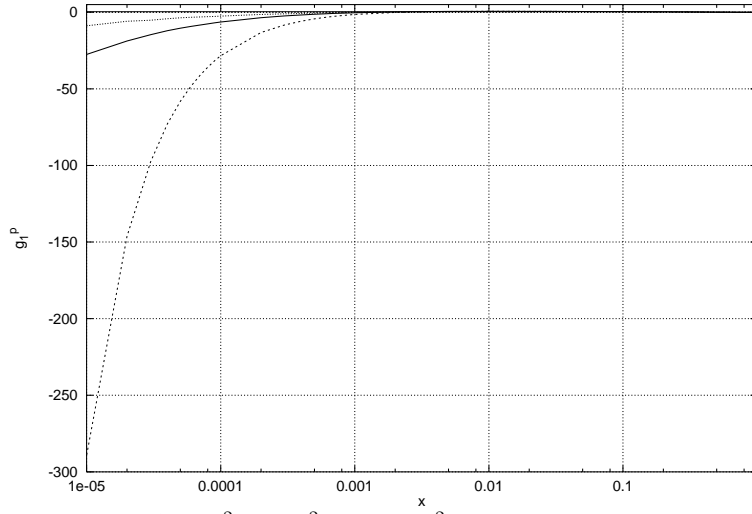


Figure 1. Structure function, $g_1^p(x, Q^2)$, at $Q^2 = 10 \text{ GeV}^2$ plotted as a function of x . Solid line corresponds to the results with the full $\ln^2(1/x)$ resummation, where the nonladder terms, ladder terms and the DGLAP kernels were included. Dotted line shows the pure DGLAP evolution. Thin solid line shows the nonperturbative input, $g_1^{(p,0)}$, and dashed line shows the incomplete DL resummation, where the nonladder terms were neglected and the DGLAP terms were included.

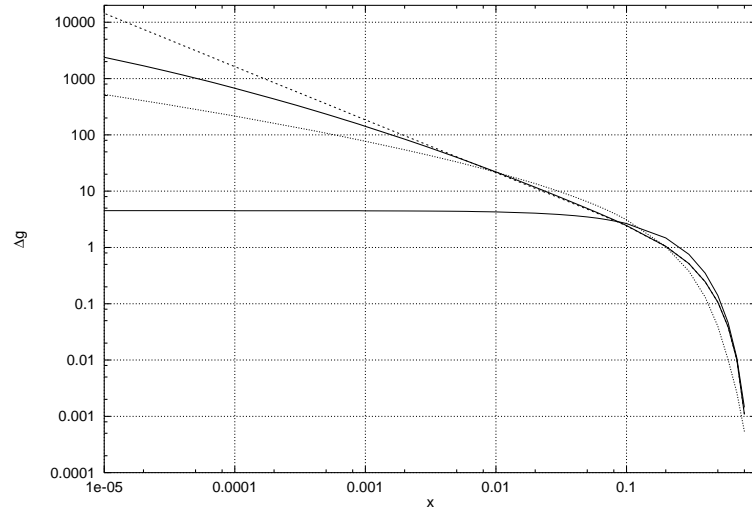


Figure 2. The spin dependent gluon distribution, $\Delta g(x, Q^2)$, at $Q^2 = 10 \text{ GeV}^2$ plotted as a function of x . Solid line corresponds to the results with the full $\ln^2(1/x)$ resummation, where the nonladder terms, ladder terms and the DGLAP kernels were included. Dotted line shows the pure DGLAP evolution. Thin solid line shows the nonperturbative input, $\Delta g^{(0)}$, and dashed line shows the incomplete DL resummation, where the nonladder terms were neglected and the DGLAP terms were included.

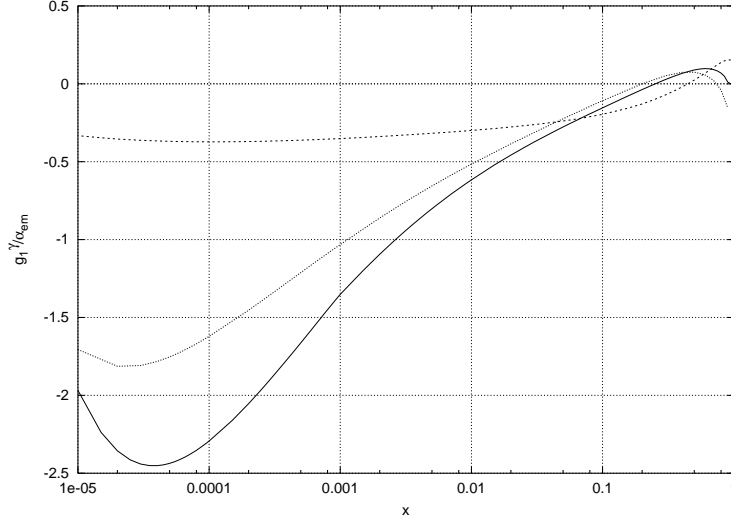


Figure 3. Structure function, $g_1^\gamma(x, Q^2)/\alpha_{em}$, at $Q^2 = 10 \text{ GeV}^2$ obtained after solving the unified evolution equations with the input parametrization (i). Solid line corresponds to the results with the full $\ln^2(1/x)$ resummation, where the nonladder, ladder corrections and the LO DGLAP kernels were included. Dashed line shows the LO DGLAP evolution, and dotted line shows the NLO DGLAP evolution.

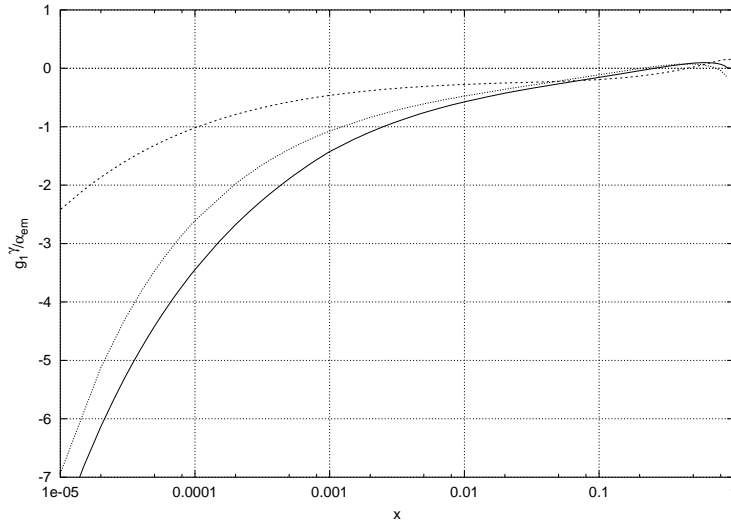


Figure 4. Structure function, $g_1^\gamma(x, Q^2)/\alpha_{em}$, at $Q^2 = 10 \text{ GeV}^2$ obtained after solving the unified evolution equations with the input parametrization (ii). Solid line corresponds to the results with the full $\ln^2(1/x)$ resummation, where the nonladder, ladder corrections and the LO DGLAP kernels were included. Dashed line shows the LO DGLAP evolution, and dotted line shows the NLO DGLAP evolution.

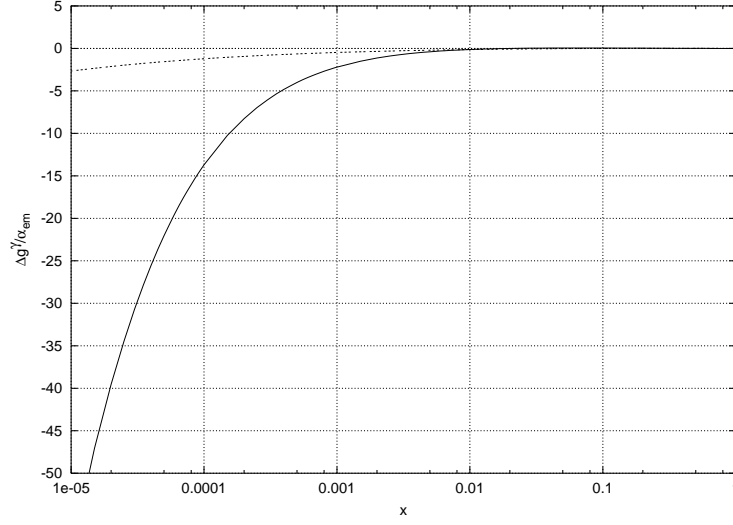


Figure 5. Spin dependent gluon distribution in photon, $\Delta g^\gamma(x, Q^2)/\alpha_{em}$, at $Q^2 = 10 \text{ GeV}^2$ obtained after solving the unified evolution equations with the input parametrization (i). Solid line corresponds to the results obtained with the full $\ln^2(1/x)$ resummation, where the nonladder, ladder corrections and the LO DGLAP kernels were included, dashed line shows the LO DGLAP evolution.

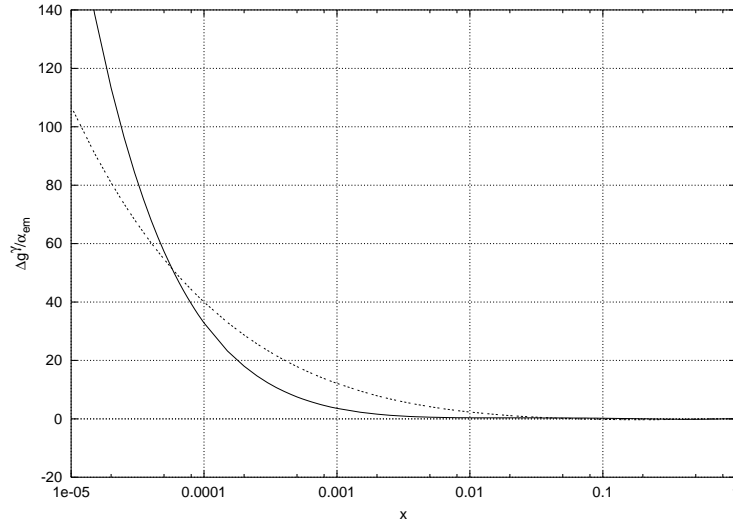


Figure 6. Spin dependent gluon distribution in photon, $\Delta g^\gamma(x, Q^2)/\alpha_{em}$, at $Q^2 = 10 \text{ GeV}^2$ obtained after solving the unified evolution equations with the input parametrization (ii). Solid line corresponds to the results obtained with the full $\ln^2(1/x)$ resummation, where the nonladder, ladder corrections and the LO DGLAP kernels were included, dashed line shows the LO DGLAP evolution.

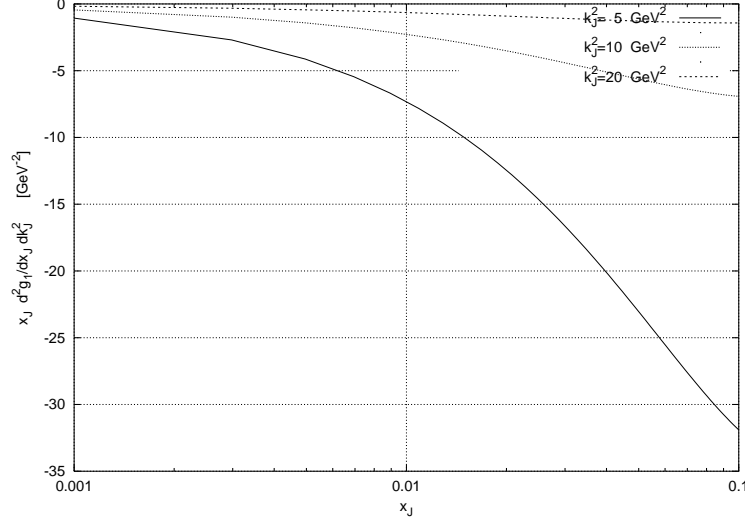


Figure 7. The differential spin structure function, $x_J \frac{\partial g_T}{\partial x_J \partial k_J^2}$, for the fixed $\bar{\alpha}_s$ (case (i)) plotted as a function of the longitudinal momentum fraction carried by a jet, x_J . We show predictions for the three different values of the transverse momentum of the jet squared, $k_J^2 = 5 \text{ GeV}^2$, 10 GeV^2 and 20 GeV^2 . Those calculations were performed at $Q^2 = 10 \text{ GeV}^2$ and $x = 10^{-4}$.

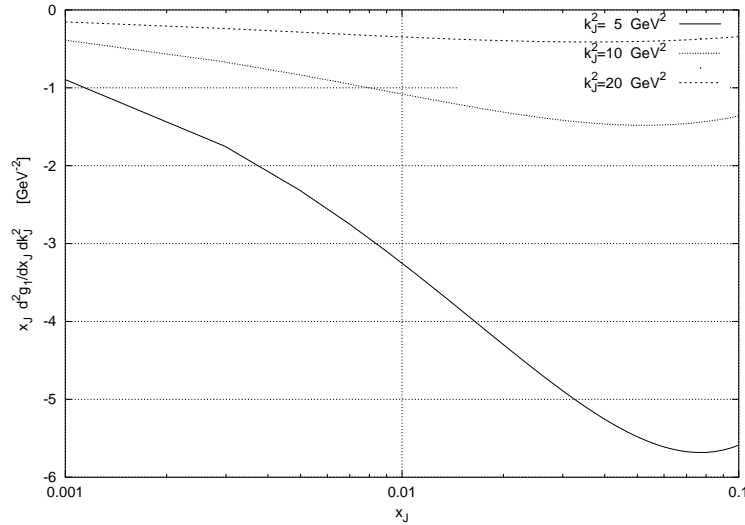


Figure 8. The differential spin structure function, $x_J \frac{\partial g_T}{\partial x_J \partial k_J^2}$, for the running $\bar{\alpha}_s$ (case (ii)) plotted as the function of the longitudinal momentum fraction carried by a jet, x_J . We show predictions for the three different values of the transverse momentum of the jet squared, $k_J^2 = 5 \text{ GeV}^2$, 10 GeV^2 and 20 GeV^2 . Those calculations were performed at $Q^2 = 10 \text{ GeV}^2$ and $x = 10^{-4}$.

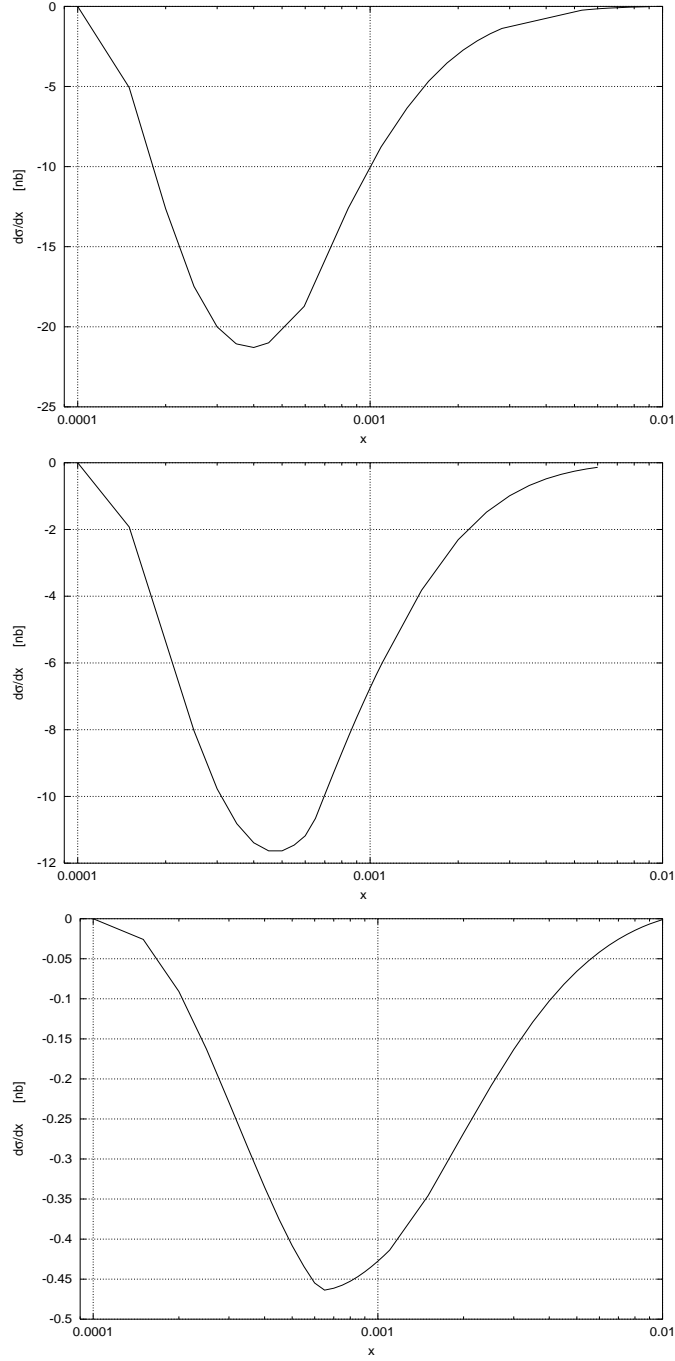


Figure 9. The cross-section, $\frac{d\sigma}{dx}$, for the forward jet production in the polarized deep inelastic scattering. Figures 2a and 2b show the results with the double logarithmic $\ln^2(1/\xi)$ effects included. They correspond to two choices of the scale μ^2 : (i) $\mu^2 = (k_f^2 + Q^2)/2$ (Fig. 2a), (ii) $\mu^2 = k_f^2/\xi$ (Fig. 2b). Fig. 2c shows the cross-section $\frac{d\sigma}{dx}$ in the Born approximation where the double logarithmic resummation was neglected.